(7) De Francesco, R.; Migliaccio, G. Challenges and successes in developing new therapies for hepatitis C. *Nature* **2005**, *436* (7053), 953–60.
(8) Kato, N.; Mori, K.; Abe, K.; Dansako, H.; Kuroki, M.; Ariumi, Y.; Wakita, T.; Ikeda, M. Efficient replication systems for hepatitis C virus using a new human hepatoma cell line. *Virus Res.* **2009**, *146* (1–2), 41–50.
(9) Murray, C. L.; Rice, C. M. Hepatitis C: An unsuspected drug target. *Nature* **2010**, *465* (7294), 42–4.
(10) Mori, Y.; Moriishi, K.; Matsuura, Y. Hepatitis C virus core protein: its coordinate roles with PA28gamma in metabolic abnormality and carcinogenicity in the liver. *Int. J. Biochem. Cell Biol.* **2008**, *40* (8), 1437–42.
(11) Gao, G.; Luo, H. The ubiquitin-proteasome pathway in viral infections. *Can. J. Physiol. Pharmacol.* **2006**, *84* (1), 5–14.
(12) Miyamoto, H.; Moriishi, K.; Moriya, K.; Murata, S.; Tanaka, K.; Suzuki, T.; Miyamura, T.; Koike, K.; Matsuura, Y. Involvement of the PA28gamma-dependent pathway in insulin resistance induced by hepatitis C virus core protein. *J. Virol.* **2007**, *81* (4), 1727–35.
(13) Moriishi, K.; Okabayashi, T.; Nakai, K.; Moriya, K.; Koike, K.; Murata, S.; Chiba, T.; Tanaka, K.; Suzuki, R.; Suzuki, T.; Miyamura, T.; Matsuura, Y. Proteasome activator PA28gamma-dependent nuclear retention and degradation of hepatitis C virus core protein. *J. Virol.* **2003**, *77* (19), 10237–49.
(14) Moriishi, K.; Shoji, I.; Mori, Y.; Suzuki, R.; Suzuki, T.; Kataoka, C.; Matsuura, Y. Involvement of PA28gamma in the propagation of hepatitis C virus. *Hepatology* **2010**, *52* (2), 411–20.
(15) Suzuki, R.; Moriishi, K.; Fukuda, K.; Shirakura, M.; Ishii, K.; Shoji, I.; Wakita, T.; Miyamura, T.; Matsuura, Y.; Suzuki, T. Proteasomal turnover of hepatitis C virus core protein is regulated by two distinct mechanisms: a ubiquitin-dependent mechanism and a ubiquitin-independent but PA28gamma-dependent mechanism. *J. Virol.* **2009**, *83* (5), 2389–92.
(16) Chen, Y. A.; Tripathi, L. P.; Mizuguchi, K. TargetMine, an integrated data warehouse for candidate gene prioritisation and target discovery. *PLoS One* **2011**, *6* (3), e17844.
(17) Liu, M. C.; Akle, V.; Zheng, W.; Dave, J. R.; Tortella, F. C.; Hayes, R. L.; Wang, K. K. Comparing calpain- and caspase-3-mediated degradation patterns in traumatic brain injury by differential proteome analysis. *Biochem. J.* **2006**, *394* (Pt 3), 715–25.
(18) Stark, C.; Breitkreutz, B. J.; Reguly, T.; Boucher, L.; Breitkreutz, A.; Tyers, M. BioGRID: a general repository for interaction datasets. *Nucleic Acids Res.* **2006**, *34* (Database issue), D535–9.
(19) Turner, B.; Razick, S.; Turinsky, A. L.; Vlasblom, J.; Crowdy, E. K.; Cho, E.; Morrison, K.; Donaldson, I. M.; Wodak, S. J. iRefWeb: interactive analysis of consolidated protein interaction data and their supporting evidence. *Database (Oxford)* **2010**, *2010*, baq023.
(20) Cline, M. S.; Smoot, M.; Cerami, E.; Kuchinsky, A.; Landys, N.; Workman, C.; Christmas, R.; Avila-Campilo, I.; Creech, M.; Gross, B.; Hanspers, K.; Isserlin, R.; Kelley, R.; Killcoyne, S.; Lotia, S.; Maere, S.; Morris, J.; Ono, K.; Pavlovic, V.; Pico, A. R.; Vailaya, A.; Wang, P. L.; Adler, A.; Conklin, B. R.; Hood, L.; Kuiper, M.; Sander, C.; Schmulevich, I.; Schwikowski, B.; Warner, G. J.; Ideker, T.; Bader, G. D. Integration of biological networks and gene expression data using Cytoscape. *Nat. Protoc.* **2007**, *2* (10), 2366–82.
(21) Assenov, Y.; Ramirez, F.; Schelhorn, S. E.; Lengauer, T.; Albrecht, M. Computing topological parameters of biological networks. *Bioinformatics* **2008**, *24* (2), 282–4.
(22) Tripathi, L. P.; Kataoka, C.; Taguwa, S.; Moriishi, K.; Mori, Y.; Matsuura, Y.; Mizuguchi, K. Network based analysis of hepatitis C virus Core and NS4B protein interactions. *Mol. Biosyst.* **2010**, *6* (12), 2539–53.
(23) Ashburner, M.; Ball, C. A.; Blake, J. A.; Botstein, D.; Butler, H.; Cherry, J. M.; Davis, A. P.; Dolinski, K.; Dwight, S. S.; Eppig, J. T.; Harris, M. A.; Hill, D. P.; Issel-Tarver, L.; Kasarskis, A.; Lewis, S.; Matese, J. C.; Richardson, J. E.; Ringwald, M.; Rubin, G. M.; Sherlock, G. Gene ontology: tool for the unification of biology. The Gene Ontology Consortium. *Nat. Genet.* **2000**, *25* (1), 25–9.
(24) Aoki-Kinoshita, K. F.; Kanehisa, M. Gene annotation and pathway mapping in KEGG. *Methods Mol. Biol.* **2007**, *396*, 71–91.
(25) McKusick-Nathans Institute of Genetic Medicine, Johns Hopkins Medicine (Baltimore, MD) and National Center for Biotechnology Information, National Library of Medicine (Bethesda, MD), Online Mendelian Inheritance in Man, OMIM (TM). In 2010.
(26) Benjamini, Y.; Hochberg, Y. Controlling the false discovery rate-A practical and powerful approach to multiple testing. *J. R. Statist. Soc. B* **1995**, *57* (1), 289–300.
(27) Noble, W. S. How does multiple testing correction work? *Nat. Biotechnol.* **2009**, *27* (12), 1135–7.
(28) Linhart, C.; Halperin, Y.; Shamir, R. Transcription factor and microRNA motif discovery: the Amadeus platform and a compendium of metazoan target sets. *Genome Res.* **2008**, *18* (7), 1180–9.
(29) Montgomery, S. B.; Griffith, O. L.; Sleumer, M. C.; Bergman, C. M.; Bilenky, M.; Pleasance, E. D.; Prychyna, Y.; Zhang, X.; Jones, S. J. ORegAnno: an open access database and curation system for literature-derived promoters, transcription factor binding sites and regulatory variation. *Bioinformatics* **2006**, *22* (5), 637–40.
(30) Okamoto, T.; Omori, H.; Kaname, Y.; Abe, T.; Nishimura, Y.; Suzuki, T.; Miyamura, T.; Yoshimori, T.; Moriishi, K.; Matsuura, Y. A single-amino-acid mutation in hepatitis C virus NS5A disrupting FKBP8 interaction impairs viral replication. *J. Virol.* **2008**, *82* (7), 3480–9.
(31) Pietschmann, T.; Lohmann, V.; Kaul, A.; Krieger, N.; Rinck, G.; Rutter, G.; Strand, D.; Bartenschlager, R. Persistent and transient replication of full-length hepatitis C virus genomes in cell culture. *J. Virol.* **2002**, *76* (8), 4008–21.
(32) Kato, T.; Date, T.; Miyamoto, M.; Furusaka, A.; Tokushige, K.; Mizokami, M.; Wakita, T. Efficient replication of the genotype 2a hepatitis C virus subgenomic replicon. *Gastroenterology* **2003**, *125* (6), 1808–17.
(33) Wakita, T.; Pietschmann, T.; Kato, T.; Date, T.; Miyamoto, M.; Zhao, Z.; Murthy, K.; Habermann, A.; Krausslich, H. G.; Mizokami, M.; Bartenschlager, R.; Liang, T. J. Production of infectious hepatitis C virus in tissue culture from a cloned viral genome. *Nat. Med.* **2005**, *11* (7), 791–6.
(34) Cao, W.; Sun, B.; Feitelson, M. A.; Wu, T.; Tur-Kaspa, R.; Fan, Q. Hepatitis C virus targets over-expression of arginase I in hepatocarcinogenesis. *Int. J. Cancer* **2009**, *124* (12), 2886–92.
(35) Tacke, R. S.; Tosello-Trampont, A.; Nguyen, V.; Mullins, D. W.; Hahn, Y. S. Extracellular hepatitis C virus core protein activates STAT3 in human monocyte/macrophage/dendritic cells via an IL-6 autocrine pathway. *J. Biol. Chem.* **2011**, DOI: 10.1074/jbc.M110.217653 .
(36) Waris, G.; Turkson, J.; Hassanein, T.; Siddiqui, A. Hepatitis C virus (HCV) constitutively activates STAT-3 via oxidative stress: role of STAT-3 in HCV replication. *J. Virol.* **2005**, *79* (3), 1569–80.
(37) Randall, G.; Panis, M.; Cooper, J. D.; Tellinghuisen, T. L.; Sukhodolets, K. E.; Pfeffer, S.; Landthaler, M.; Landgraf, P.; Kan, S.; Lindenbach, B. D.; Chien, M.; Weir, D. B.; Russo, J. J.; Ju, J.; Brownstein, M. J.; Sheridan, R.; Sander, C.; Zavolan, M.; Tuschl, T.; Rice, C. M. Cellular cofactors affecting hepatitis C virus infection and replication. *Proc. Natl. Acad. Sci. U.S.A.* **2007**, *104* (31), 12884–9.
(38) Lin, W.; Kim, S. S.; Yeung, E.; Kamegaya, Y.; Blackard, J. T.; Kim, K. A.; Holtzman, M. J.; Chung, R. T. Hepatitis C virus core protein blocks interferon signaling by interaction with the STAT1 SH2 domain. *J. Virol.* **2006**, *80* (18), 9226–35.
(39) Tsutsumi, T.; Suzuki, T.; Moriya, K.; Shintani, Y.; Fujie, H.; Miyoshi, H.; Matsuura, Y.; Koike, K.; Miyamura, T. Hepatitis C virus core protein activates ERK and p38 MAPK in cooperation with ethanol in transgenic mice. *Hepatology* **2003**, *38* (4), 820–8.
(40) Nanda, S. K.; Herion, D.; Liang, T. J. The SH3 binding motif of HCV [corrected] NS5A protein interacts with Bin1 and is important for apoptosis and infectivity. *Gastroenterology* **2006**, *130* (3), 794–809.
(41) Jacobs, J. M.; Diamond, D. L.; Chan, E. Y.; Gritsenko, M. A.; Qian, W.; Stastna, M.; Baas, T.; Camp, D. G., 2nd; Carithers, R. L., Jr.; Smith, R. D.; Katze, M. G. Proteome analysis of liver cells expressing a full-length hepatitis C virus (HCV) replicon and biopsy specimens of

posttransplantation liver from HCV-infected patients. *J. Virol.* **2005**, *79* (12), 7558–69.
(42) Woodhouse, S. D.; Narayan, R.; Latham, S.; Lee, S.; Antrobus, R.; Gangadharan, B.; Luo, S.; Schroth, G. P.; Klenerman, P.; Zitzmann, N. Transcriptome sequencing, microarray, and proteomic analyses reveal cellular and metabolic impact of hepatitis C virus infection in vitro. *Hepatology* **2010**, *52* (2), 443–53.
(43) Fujino, T.; Nakamuta, M.; Yada, R.; Aoyagi, Y.; Yasutake, K.; Kohjima, M.; Fukuizumi, K.; Yoshimoto, T.; Harada, N.; Yada, M.; Kato, M.; Kotoh, K.; Taketomi, A.; Maehara, Y.; Nakashima, M.; Enjoji, M. Expression profile of lipid metabolism-associated genes in hepatitis C virus-infected human liver. *Hepatol. Res.* **2010**, *40* (9), 923–9.
(44) MacPherson, J. I.; Sidders, B.; Wieland, S.; Zhong, J.; Targett-Adams, P.; Lohmann, V.; Backes, P.; Delpuech-Adams, O.; Chisari, F.; Lewis, M.; Parkinson, T.; Robertson, D. L. An integrated transcriptomic and meta-analysis of hepatoma cells reveals factors that influence susceptibility to HCV infection. *PLoS One* **2011**, *6* (10), e25584.
(45) de Chassey, B.; Navratil, V.; Tafforeau, L.; Hiet, M. S.; Aublin-Gex, A.; Agaugue, S.; Meiffren, G.; Pradezynski, F.; Faria, B. F.; Chantier, T.; Le Breton, M.; Pellet, J.; Davoust, N.; Mangeot, P. E.; Chaboud, A.; Penin, F.; Jacob, Y.; Vidalain, P. O.; Vidal, M.; Andre, P.; Rabourdin-Combe, C.; Lotteau, V. Hepatitis C virus infection protein network. *Mol. Syst. Biol.* **2008**, *4*, 230.
(46) Chazal, N.; Gerlier, D. Virus entry, assembly, budding, and membrane rafts. *Microbiol. Mol. Biol. Rev.* **2003**, *67* (2), 226–37.
(47) Manes, S.; del Real, G.; Martinez, A. C. Pathogens: raft hijackers. *Nat. Rev. Immunol.* **2003**, *3* (7), 557–68.
(48) Riethmuller, J.; Riehle, A.; Grassme, H.; Gulbins, E. Membrane rafts in host-pathogen interactions. *Biochim. Biophys. Acta* **2006**, *1758* (12), 2139–47.
(49) Suzuki, T.; Suzuki, Y. Virus infection and lipid rafts. *Biol. Pharm. Bull.* **2006**, *29* (8), 1538–41.
(50) Mannova, P.; Fang, R.; Wang, H.; Deng, B.; McIntosh, M. W.; Hanash, S. M.; Beretta, L. Modification of host lipid raft proteome upon hepatitis C virus replication. *Mol. Cell. Proteomics* **2006**, *5* (12), 2319–25.
(51) Corless, L.; Crump, C. M.; Griffin, S. D.; Harris, M. Vps4 and the ESCRT-III complex are required for the release of infectious hepatitis C virus particles. *J. Gen. Virol.* **2010**, *91* (Pt 2), 362–72.
(52) Lai, C. K.; Jeng, K. S.; Machida, K.; Lai, M. M. Hepatitis C virus egress and release depend on endosomal trafficking of core protein. *J. Virol.* **2010**, *84* (21), 11590–8.
(53) Jahn, R.; Scheller, R. H. SNAREs—engines for membrane fusion. *Nat. Rev. Mol. Cell. Biol.* **2006**, *7* (9), 631–43.
(54) Kreykenbohm, V.; Wenzel, D.; Antonin, W.; Atlachkine, V.; von Mollard, G. F. The SNAREs vti1a and vti1b have distinct localization and SNARE complex partners. *Eur. J. Cell Biol.* **2002**, *81* (5), 273–80.
(55) Kunwar, A. J.; Rickmann, M.; Backofen, B.; Browski, S. M.; Rosenbusch, J.; Schoning, S.; Fleischmann, T.; Krieglstein, K.; Fischer von Mollard, G. Lack of the endosomal SNAREs vti1a and vti1b led to significant impairments in neuronal development. *Proc. Natl. Acad. Sci. U.S.A.* **2011**, *108* (6), 2575–80.
(56) Mascia, L.; Langosch, D. Evidence that late-endosomal SNARE multimerization complex is promoted by transmembrane segments. *Biochim. Biophys. Acta* **2007**, *1768* (3), 457–66.
(57) Offenhauser, C.; Lei, N.; Roy, S.; Collins, B. M.; Stow, J. L.; Murray, R. Z. Syntaxin 11 binds Vti1b and regulates late endosome to lysosome fusion in macrophages. *Traffic* **2011**, *12*, 762–73.
(58) Bryceson, Y. T.; Chiang, S. C.; Darmanin, S.; Fauriat, C.; Schlums, H.; Theorell, J.; Wood, S. M. Molecular mechanisms of natural killer cell activation. *J. Innate Immun.* **2011**, *3* (3), 216–26.
(59) Arneson, L. N.; Brickshawana, A.; Segovis, C. M.; Schoon, R. A.; Dick, C. J.; Leibson, P. J. Cutting edge: syntaxin 11 regulates lymphocyte-mediated secretion and cytotoxicity. *J. Immunol.* **2007**, *179* (6), 3397–401.
(60) Dabrazhynetskaya, A.; Ma, J.; Guerreiro-Cacais, A. O.; Arany, Z.; Rudd, E.; Henter, J. I.; Karre, K.; Levitskaya, J.; Levitsky, V. Syntaxin 11 marks a distinct intracellular compartment recruited to the immunological synapse of NK cells to co-localize with cytotoxic granules. *J. Cell. Mol. Med.* **2011**, *16*, 129–41.
(61) Gholam, C.; Grigoriadou, S.; Gilmour, K. C.; Gaspar, H. B. Familial haemophagocytic lymphohistiocytosis: advances in the genetic basis, diagnosis and management. *Clin. Exp. Immunol.* **2011**, *163* (3), 271–83.
(62) How, P. C.; Shields, D. Tethering function of the caspase cleavage fragment of Golgi protein p115 promotes apoptosis via a p53-dependent pathway. *J. Biol. Chem.* **2011**, *286* (10), 8565–76.
(63) Radulescu, A. E.; Mukherjee, S.; Shields, D. The Golgi protein p115 associates with gamma-tubulin and plays a role in Golgi structure and mitosis progression. *J. Biol. Chem.* **2011**, *286* (24), 21915–26.
(64) Bouffard, P.; Hayashi, P. H.; Acevedo, R.; Levy, N.; Zeldis, J. B. Hepatitis C virus is detected in a monocyte/macrophage subpopulation of peripheral blood mononuclear cells of infected patients. *J. Infect. Dis.* **1992**, *166* (6), 1276–80.
(65) Roxrud, I.; Raiborg, C.; Pedersen, N. M.; Stang, E.; Stenmark, H. An endosomally localized isoform of Eps15 interacts with Hrs to mediate degradation of epidermal growth factor receptor. *J. Cell Biol.* **2008**, *180* (6), 1205–18.
(66) Salcini, A. E.; Chen, H.; Iannolo, G.; De Camilli, P.; Di Fiore, P. P. Epidermal growth factor pathway substrate 15, Eps15. *Int. J. Biochem. Cell Biol.* **1999**, *31* (8), 805–9.
(67) Barnaba, V. Hepatitis C virus infection: a "liaison a trois" amongst the virus, the host, and chronic low-level inflammation for human survival. *J. Hepatol.* **2010**, *53* (4), 752–61.
(68) Hiroishi, K.; Ito, T.; Imawari, M. Immune responses in hepatitis C virus infection and mechanisms of hepatitis C virus persistence. *J. Gastroenterol. Hepatol.* **2008**, *23* (10), 1473–82.
(69) Kawai, T.; Akira, S. Toll-like receptor and RIG-I-like receptor signaling. *Ann. N.Y. Acad. Sci.* **2008**, *1143*, 1–20.
(70) Sklan, E. H.; Charuworn, P.; Pang, P. S.; Glenn, J. S. Mechanisms of HCV survival in the host. *Nat. Rev. Gastroenterol. Hepatol.* **2009**, *6* (4), 217–27.
(71) Szabo, G.; Dolganiuc, A. Hepatitis C and innate immunity: recent advances. *Clin. Liver Dis.* **2008**, *12* (3), 675–92.
(72) Taylor, D. R.; Silberstein, E. Innate immunity and hepatitis C virus: eluding the host cell defense. *Front. Biosci.* **2009**, *14*, 4950–61.
(73) Legarda-Addison, D.; Hase, H.; O'Donnell, M. A.; Ting, A. T. NEMO/IKKgamma regulates an early NF-kappaB-independent cell-death checkpoint during TNF signaling. *Cell Death Differ.* **2009**, *16* (9), 1279–88.
(74) Ye, X.; Lu, H.; Huo, K.; Chen, D. Finding a novel interacting protein of the hepatic carcinoma related gene MIP: NF-kappaB essential modulator (NEMO). *Oncol. Rep.* **2011**, *25* (1), 231–5.
(75) Beraza, N.; Malato, Y.; Sander, L. E.; Al-Masaoudi, M.; Freimuth, J.; Riethmacher, D.; Gores, G. J.; Roskams, T.; Liedtke, C.; Trautwein, C. Hepatocyte-specific NEMO deletion promotes NK/NKT cell- and TRAIL-dependent liver damage. *J. Exp. Med.* **2009**, *206* (8), 1727–37.
(76) Cruz-Munoz, M. E.; Veillette, A. Do NK cells always need a license to kill? *Nat. Immunol.* **2010**, *11* (4), 279–80.
(77) Wang, K.; Song, Y.; Chen, D. B.; Zheng, J. Protein phosphatase 3 differentially modulates vascular endothelial growth factor- and fibroblast growth factor 2-stimulated cell proliferation and signaling in ovine fetoplacental artery endothelial cells. *Biol. Reprod.* **2008**, *79* (4), 704–10.
(78) Singh, A. P.; Bafna, S.; Chaudhary, K.; Venkatraman, G.; Smith, L.; Eudy, J. D.; Johansson, S. L.; Lin, M. F.; Batra, S. K. Genome-wide expression profiling reveals transcriptomic variation and perturbed gene networks in androgen-dependent and androgen-independent prostate cancer cells. *Cancer Lett.* **2008**, *259* (1), 28–38.
(79) Ostenfeld, M. S.; Bramsen, J. B.; Lamy, P.; Villadsen, S. B.; Fristrup, N.; Sorensen, K. D.; Ulhoi, B.; Borre, M.; Kjems, J.; Dyrskjot, L.; Orntoft, T. F. miR-145 induces caspase-dependent and -independent cell death in urothelial cancer cell lines with targeting of an expression signature present in Ta bladder tumors. *Oncogene* **2010**, *29* (7), 1073–84.

(80) Johansen, C.; Vestergaard, C.; Kragballe, K.; Kollias, G.; Gaestel, M.; Iversen, L. MK2 regulates the early stages of skin tumor promotion. *Carcinogenesis* **2009**, *30* (12), 2100–8.
(81) Wang, C.; Zhou, J.; Wang, S.; Ye, M.; Fan, G.; Zou, H.; Jiang, C. Shotgun approach based comparative proteomic analysis of levo-tetrahydropalmatine-induced apoptosis in hepatocytes. *Toxicol. Lett.* **2010**, *194* (1–2), 8–15.
(82) Del Campo, J. A.; Romero-Gomez, M. Steatosis and insulin resistance in hepatitis C: a way out for the virus? *World J. Gastroenterol.* **2009**, *15* (40), 5014–9.
(83) Douglas, M. W.; George, J. Molecular mechanisms of insulin resistance in chronic hepatitis C. *World J. Gastroenterol.* **2009**, *15* (35), 4356–64.
(84) Shintani, Y.; Fujie, H.; Miyoshi, H.; Tsutsumi, T.; Tsukamoto, K.; Kimura, S.; Moriya, K.; Koike, K. Hepatitis C virus infection and diabetes: direct involvement of the virus in the development of insulin resistance. *Gastroenterology* **2004**, *126* (3), 840–8.
(85) Cao, X.; Pobezinskaya, Y. L.; Morgan, M. J.; Liu, Z. G. The role of TRADD in TRAIL-induced apoptosis and signaling. *FASEB J.* **2011**, *25* (4), 1353–8.
(86) Zheng, L.; Bidere, N.; Staudt, D.; Cubre, A.; Orenstein, J.; Chan, F. K.; Lenardo, M. Competitive control of independent programs of tumor necrosis factor receptor-induced cell death by TRADD and RIP1. *Mol. Cell. Biol.* **2006**, *26* (9), 3505–13.
(87) Tellinghuisen, T. L.; Foss, K. L.; Treadaway, J. Regulation of hepatitis C virion production via phosphorylation of the NS5A protein. *PLoS Pathog.* **2008**, *4* (3), e1000032.
(88) Benedicto, I.; Molina-Jimenez, F.; Bartosch, B.; Cosset, F. L.; Lavillette, D.; Prieto, J.; Moreno-Otero, R.; Valenzuela-Fernandez, A.; Aldabe, R.; Lopez-Cabrera, M.; Majano, P. L. The tight junction-associated protein occludin is required for a postbinding step in hepatitis C virus entry and infection. *J. Virol.* **2009**, *83* (16), 8012–20.
(89) Bantel, H.; Schulze-Osthoff, K. Apoptosis in hepatitis C virus infection. *Cell Death Differ.* **2003**, *10* (Suppl 1), S48–58.
(90) Deng, L.; Adachi, T.; Kitayama, K.; Bungyoku, Y.; Kitazawa, S.; Ishido, S.; Shoji, I.; Hotta, H. Hepatitis C virus infection induces apoptosis through a Bax-triggered, mitochondrion-mediated, caspase 3-dependent pathway. *J. Virol.* **2008**, *82* (21), 10375–85.
(91) Fischer, R.; Baumert, T.; Blum, H. E. Hepatitis C virus infection and apoptosis. *World J. Gastroenterol.* **2007**, *13* (36), 4865–72.
(92) Hanafy, S. M.; Shehata, O. H.; Farahat, N. M. Expression of apoptotic markers BCL-2 and Bax in chronic hepatitis C virus patients. *Clin. Biochem.* **2010**, *43* (13–14), 1112–7.
(93) Joyce, M. A.; Walters, K. A.; Lamb, S. E.; Yeh, M. M.; Zhu, L. F.; Kneteman, N.; Doyle, J. S.; Katze, M. G.; Tyrrell, D. L. HCV induces oxidative and ER stress, and sensitizes infected cells to apoptosis in SCID/Alb-uPA mice. *PLoS Pathog.* **2009**, *5* (2), e1000291.
(94) Kondo, Y.; Machida, K.; Liu, H. M.; Ueno, Y.; Kobayashi, K.; Wakita, T.; Shimosegawa, T.; Lai, M. M. Hepatitis C virus infection of T cells inhibits proliferation and enhances fas-mediated apoptosis by down-regulating the expression of CD44 splicing variant 6. *J. Infect. Dis.* **2009**, *199* (5), 726–36.
(95) Anupam, R.; Datta, A.; Kesic, M.; Green-Church, K.; Shkriabai, N.; Kvaratskhelia, M.; Lairmore, M. D. Human T-lymphotropic virus type 1 p30 interacts with REGgamma and modulates ATM (ataxia telangiectasia mutated) to promote cell survival. *J. Biol. Chem.* **2011**, *286* (9), 7661–8.
(96) Mao, I.; Liu, J.; Li, X.; Luo, H. REGgamma, a proteasome activator and beyond? *Cell. Mol. Life Sci.* **2008**, *65* (24), 3971–80.
(97) Tian, M.; Xiaoyi, W.; Xiaotao, L.; Guosheng, R. Proteasomes reactivator REG gamma enchances oncogenicity of MDA-MB-231 cell line via promoting cell proliferation and inhibiting apoptosis. *Cell. Mol. Biol. (Noisy-le-Grand)* **2009**, *55* (Suppl), OL1121–31.
(98) Zannini, L.; Buscemi, G.; Fontanella, E.; Lisanti, S.; Delia, D. REGgamma/PA28gamma proteasome activator interacts with PML and Chk2 and affects PML nuclear bodies number. *Cell Cycle* **2009**, *8* (15), 2399–407.
(99) Samuelsen, J. T.; Schwarze, P. E.; Huitfeldt, H. S.; Thrane, E. V.; Lag, M.; Refsnes, M.; Skarpen, E.; Becher, R. Regulation of rat alveolar type 2 cell proliferation in vitro involves type II cAMP-dependent protein kinase. *Am. J. Physiol. Lung Cell. Mol. Physiol.* **2007**, *292* (1), L232–9.
(100) Bungyoku, Y.; Shoji, I.; Makine, T.; Adachi, T.; Hayashida, K.; Nagano-Fujii, M.; Ide, Y. H.; Deng, L.; Hotta, H. Efficient production of infectious hepatitis C virus with adaptive mutations in cultured hepatoma cells. *J. Gen. Virol.* **2009**, *90* (Pt 7), 1681–91.
(101) Lemon, S. M.; McKeating, J. A.; Pietschmann, T.; Frick, D. N.; Glenn, J. S.; Tellinghuisen, T. L.; Symons, J.; Furman, P. A. Development of novel therapies for hepatitis C. *Antiviral Res.* **2010**, *86* (1), 79–92.
(102) Lin, K. Development of novel antiviral therapies for hepatitis C virus. *Virol. Sin.* **2010**, *25* (4), 246–66.
(103) Chan, S. C.; Lo, S. Y.; Liou, J. W.; Lin, M. C.; Syu, C. L.; Lai, M. J.; Chen, Y. C.; Li, H. C. Visualization of the structures of the hepatitis C virus replication complex. *Biochem. Biophys. Res. Commun.* **2011**, *404* (1), 574–8.
(104) Dreyer, J. L. Lentiviral vector-mediated gene transfer and RNA silencing technology in neuronal dysfunctions. *Mol. Biotechnol.* **2011**, *47* (2), 169–87.
(105) Camm, E. J.; Martin-Gronert, M. S.; Wright, N. L.; Hansell, J. A.; Ozanne, S. E.; Giussani, D. A. Prenatal hypoxia independent of undernutrition promotes molecular markers of insulin resistance in adult offspring. *FASEB J.* **2011**, *25* (1), 420–7.
(106) Ning, B. F.; Ding, J.; Yin, C.; Zhong, W.; Wu, K.; Zeng, X.; Yang, W.; Chen, Y. X.; Zhang, J. P.; Zhang, X.; Wang, H. Y.; Xie, W. F. Hepatocyte nuclear factor 4 alpha suppresses the development of hepatocellular carcinoma. *Cancer Res.* **2010**, *70* (19), 7640–51.
(107) Niehof, M.; Borlak, J. EPS15R, TASP1, and PRPF3 are novel disease candidate genes targeted by HNF4alpha splice variants in hepatocellular carcinomas. *Gastroenterology* **2008**, *134* (4), 1191–202.
(108) Hussain, K. M.; Leong, K. L.; Ng, M. M.; Chu, J. J. The essential role of clathrin-mediated endocytosis in the infectious entry of human enterovirus 71. *J. Biol. Chem.* **2011**, *286* (1), 309–21.
(109) Helle, F.; Dubuisson, J. Hepatitis C virus entry into host cells. *Cell. Mol. Life Sci.* **2008**, *65* (1), 100–12.
(110) Marshall, A.; Rushbrook, S.; Morris, L. S.; Scott, I. S.; Vowler, S. L.; Davies, S. E.; Coleman, N.; Alexander, G. Hepatocyte expression of minichromosome maintenance protein-2 predicts fibrosis progression after transplantation for chronic hepatitis C virus: a pilot study. *Liver Transpl.* **2005**, *11* (4), 427–33.
(111) Bard-Chapeau, E. A.; Li, S.; Ding, J.; Zhang, S. S.; Zhu, H. H.; Princen, F.; Fang, D. D.; Han, T.; Bailly-Maitre, B.; Poli, V.; Varki, N. M.; Wang, H.; Feng, G. S. Ptpn11/Shp2 acts as a tumor suppressor in hepatocellular carcinogenesis. *Cancer Cell* **2011**, *19* (5), 629–39.
(112) Matsuo, K.; Delibegovic, M.; Matsuo, I.; Nagata, N.; Liu, S.; Bettaieb, A.; Xi, Y.; Araki, K.; Yang, W.; Kahn, B. B.; Neel, B. G.; Haj, F. G. Altered glucose homeostasis in mice with liver-specific deletion of Src homology phosphatase 2. *J. Biol. Chem.* **2010**, *285* (51), 39750–8.
(113) Rios, E. J.; Piliponsky, A. M.; Ra, C.; Kalesnikoff, J.; Galli, S. J. Rabaptin-5 regulates receptor expression and functional activation in mast cells. *Blood* **2008**, *112* (10), 4148–57.
(114) Stenmark, H.; Vitale, G.; Ullrich, O.; Zerial, M. Rabaptin-5 is a direct effector of the small GTPase Rab5 in endocytic membrane fusion. *Cell* **1995**, *83* (3), 423–32.
(115) Edamoto, Y.; Hara, A.; Biernat, W.; Terracciano, L.; Cathomas, G.; Riehle, H. M.; Matsuda, M.; Fujii, H.; Scoazec, J. Y.; Ohgaki, H. Alterations of RB1, p53 and Wnt pathways in hepatocellular carcinomas associated with hepatitis C, hepatitis B and alcoholic liver cirrhosis. *Int. J. Cancer* **2003**, *106* (3), 334–41.
(116) Laurent-Puig, P.; Zucman-Rossi, J. Genetics of hepatocellular tumors. *Oncogene* **2006**, *25* (27), 3778–86.
(117) Park, K. J.; Choi, S. H.; Koh, M. S.; Kim, D. J.; Yie, S. W.; Lee, S. Y.; Hwang, S. B. Hepatitis C virus core protein potentiates c-Jun N-terminal kinase activation through a signaling complex involving TRADD and TRAF2. *Virus Res.* **2001**, *74* (1–2), 89–98.
(118) Kawaguchi, T.; Yoshida, T.; Harada, M.; Hisamoto, T.; Nagao, Y.; Ide, T.; Taniguchi, E.; Kumemura, H.; Hanada, S.; Maeyama, M.;

Baba, S.; Koga, H.; Kumashiro, R.; Ueno, T.; Ogata, H.; Yoshimura, A.; Sata, M. Hepatitis C virus down-regulates insulin receptor substrates 1 and 2 through up-regulation of suppressor of cytokine signaling 3. *Am. J. Pathol.* **2004**, *165* (5), 1499–508.

(119) Ma, Z.; Liu, Z.; Wu, R. F.; Terada, L. S. p66(Shc) restrains Ras hyperactivation and suppresses metastatic behavior. *Oncogene* **2010**, *29* (41), 5559–67.

(120) Spoden, G. A.; Rostek, U.; Lechner, S.; Mitterberger, M.; Mazurek, S.; Zwerschke, W. Pyruvate kinase isoenzyme M2 is a glycolytic sensor differentially regulating cell proliferation, cell size and apoptotic cell death dependent on glucose supply. *Exp. Cell Res.* **2009**, *315* (16), 2765–74.

JVI
Journals.ASM.org

Expression of MicroRNA miR-122 Facilitates an Efficient Replication in Nonhepatic Cells upon Infection with Hepatitis C Virus

Takasuke Fukuhara,[a] Hiroto Kambara,[a] Mai Shiokawa,[a] Chikako Ono,[a] Hiroshi Katoh,[a] Eiji Morita,[a] Daisuke Okuzaki,[b] Yoshihiko Maehara,[c] Kazuhiko Koike,[d] and Yoshiharu Matsuura[a]

Department of Molecular Virology[a] and DNA-Chip Developmental Center for Infectious Diseases,[b] Research Institute for Microbial Diseases, Osaka University, Osaka, Japan; Department of Surgery and Science, Graduate School of Medical Sciences, Kyushu University, Fukuoka, Japan[c]; and Department of Gastroenterology, Graduate School of Medicine, University of Tokyo, Tokyo, Japan[d]

Hepatitis C virus (HCV) is one of the most common etiologic agents of chronic liver diseases, including liver cirrhosis and hepatocellular carcinoma. In addition, HCV infection is often associated with extrahepatic manifestations (EHM), including mixed cryoglobulinemia and non-Hodgkin's lymphoma. However, the mechanisms of cell tropism of HCV and HCV-induced EHM remain elusive, because *in vitro* propagation of HCV has been limited in the combination of cell culture-adapted HCV (HCVcc) and several hepatic cell lines. Recently, a liver-specific microRNA called miR-122 was shown to facilitate the efficient propagation of HCVcc in several hepatic cell lines. In this study, we evaluated the importance of miR-122 on the replication of HCV in nonhepatic cells. Among the nonhepatic cell lines expressing functional HCV entry receptors, Hec1B cells derived from human uterus exhibited a low level of replication of the HCV genome upon infection with HCVcc. Exogenous expression of miR-122 in several cells facilitates efficient viral replication but not production of infectious particles, probably due to the lack of hepatocytic lipid metabolism. Furthermore, expression of mutant miR-122 carrying a substitution in a seed domain was required for efficient replication of mutant HCVcc carrying complementary substitutions in miR-122-binding sites, suggesting that specific interaction between miR-122 and HCV RNA is essential for the enhancement of viral replication. In conclusion, although miR-122 facilitates efficient viral replication in nonhepatic cells, factors other than miR-122, which are most likely specific to hepatocytes, are required for HCV assembly.

More than 170 million individuals worldwide are infected with hepatitis C virus (HCV), and cirrhosis and hepatocellular carcinoma induced by HCV infection are life-threatening diseases (57). Although therapy combining pegylated interferon (IFN) and ribavirin has achieved a sustained virological response in 50% of individuals infected with HCV genotype 1 (37), a more effective therapeutic modality for HCV infection is needed (46). The establishment of *in vivo* and *in vitro* infection systems has been hampered by the narrow host range and tissue tropism of HCV. Although the chimpanzee is the only experimental animal susceptible to HCV infection, it is difficult to use the chimpanzee in experiments due to ethical concerns (3). Furthermore, robust *in vitro* HCV propagation is limited to the combination of cell culture-adapted clones based on the genotype 2a JFH1 strain (HCVcc) and human hepatoma cell lines, including Huh7, Hep3B, and HepG2 (29, 43, 62).

It is well-known that HCV mainly infects hepatocytes. However, the precise mechanism underlying the liver tropism of HCV has not been clarified. Chronic hepatitis C virus infection is often associated with at least one extrahepatic manifestation (EHM), including mixed cryoglobulinemia, non-Hodgkin's lymphoma, lichen planus, thyroiditis, diabetes mellitus, Sjögren syndrome, and arthritis (19). EHMs are frequently more serious than hepatic disease in some patients and sometimes occur even in patients with persistently normal liver functions (19). Mixed cryoglobulinemia is the most-well-characterized HCV-associated disease and is curable by viral clearance through antiviral therapies (6). Although replication of HCV RNA in peripheral blood mononuclear cells (PBMCs) and neuronal cells at a low level was suggested (64), the biological significance of the extrahepatic replication of HCV, particularly in the development of EHMs, is not well understood.

MicroRNAs (miRNAs) are small noncoding RNAs consisting of 20 to 25 nucleotides that modulate gene expression in plants and animals (1, 24). Most miRNAs negatively regulate translation through the interaction with the 3′ untranslated region (UTR) of mRNA in a sequence-specific manner. miRNA 122 (miR-122) is liver specific, is the most abundantly expressed miRNA in the liver, and represses the translation of several mRNAs (5, 7). Jopling et al. reported for the first time that the inhibition of miR-122 dramatically decreased RNA replication in HCV subgenomic replicon (SGR) cells (28). In addition, several reports revealed that a specific interaction between the seed domain of miR-122 and the complementary sequences in the 5′ UTR of HCV RNA is essential for the enhancement of translation and replication of the HCV genome (21, 25, 27, 36). Endogenous expression levels of miR-122 are significantly higher in Huh7 cells than in other hepatic and nonhepatic cell lines (Fig. 1). In addition, previous reports showed that miR-122 expression enhanced the replication of SGR RNA in human embryonic kidney 293 (HEK293) cells and mouse embryonic fibroblasts (MEFs) (8, 35). Furthermore, it was recently shown that exogenous expression of miR-122 facilitates the efficient propagation of HCVcc in Hep3B and HepG2 cells, which are

Received 4 March 2012 Accepted 10 May 2012
Published ahead of print 16 May 2012
Address correspondence to Yoshiharu Matsuura, matsuura@biken.osaka-u.ac.jp.

doi:10.1128/JVI.00567-12

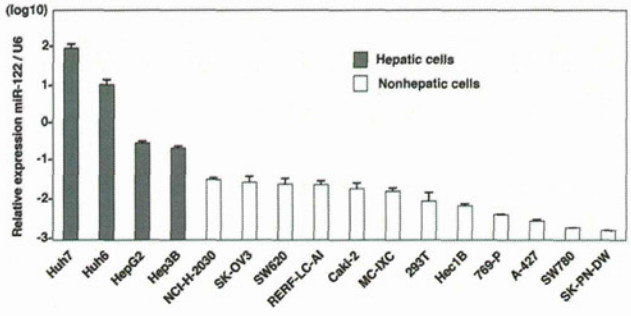

FIG 1 Endogenous expression levels of miR-122 in hepatic and nonhepatic cells. Total miRNAs were extracted from Huh7, Huh6, HepG2, Hep3B, NCI-H-2030, SK-OV3, SW620, RERF-LC-AI, Caki-2, MC-IXC, 293T, Hec1B, 769-P, A-427, SW780, and SK-PN-DW cells, and the expression levels of miR-122 were determined by qRT-PCR.

nonpermissive for HCVcc propagation (29, 43). These results suggest that the high susceptibility of Huh7 cells to the propagation of HCVcc is attributable to the high expression level of miR-122 and raise the possibility of expanding the HCV host range through the exogenous expression of miR-122 in nonhepatic cells.

In this study, we assessed the effect of miR-122 expression on the replication of HCVcc and SGR RNA in several nonhepatic cell lines. Although the exogenous expression of miR-122 in the cell lines facilitates significant RNA replication through a gene-specific interaction between miR-122 and 5′ UTR of HCV RNA, no infectivity was detected in either the cells or the culture supernatants. The current study suggests that the expression of miR-122 plays an important role in HCV cell tropism, as well as in the possible involvement of nonhepatic cells in EHM, through an incomplete propagation of HCV.

MATERIALS AND METHODS

NextBio Body Atlas. The NextBio Body Atlas application presents an aggregated analysis of gene expression across various normal tissues, normal cell types, and cancer cell lines. It enables us to investigate the expression of individual genes as well as gene sets. Samples for Body Atlas data are obtained from publicly available studies that are internally curated, annotated, and processed (31). Body Atlas measurements are generated from all available RNA expression studies that used Affymetrix U133 Plus or U133A Genechip arrays for human studies. The results corresponding to 128 human tissue samples were incorporated from 1,067 arrays, the results corresponding to 157 human cell types were incorporated from 1,474 arrays, and the results corresponding to 359 human cancer cell lines were incorporated from 376 arrays. Gene queries return a list of relevant tissues or cell types rank ordered by absolute gene expression and grouped by body systems or across all body systems. In the current analysis, we screened for nonhepatic cell lines expressing HCV receptor candidates, including CD81, SR-BI, claudin1 (CLDN1), and occludin (OCLN), or very-low-density lipoprotein (VLDL)-associated proteins, including apolipoprotein E (ApoE), ApoB, and microsomal triglyceride transfer protein (MTTP). A detailed analysis protocol developed by NextBio was described previously (31). The raw data used in this application are derived from the GSK Cancer Cell Line data deposited at the National Cancer Institute website (https://array.nci.nih.gov/caarray/project/woost-00041) and additionally from NCBI Gene Expression Omnibus (GEO) accession number GSE5720 for cell lines SK-OV-3 and SW620.

Sample collection and RNA extraction for microarray analysis. Total RNAs extracted from cells were purified by using an miRNeasy kit (Qiagen, Valencia, CA) according to the manufacturer's protocol. Eluted RNAs were quantified using a Nanodrop ND-1000 (version 3.5.2) spectrophotometer (Thermo Scientific, Wartham, MA). RNA integrity was evaluated using the RNA 6000 LabChip kit and bioanalyzer (Agilent Technologies, Santa Clara, CA). Each RNA that had an RNA integrity number (RIN) greater than 9.0 was used for the microarray experiments.

Microarray experiment. Expression profiling was generated using the 4 × 44K whole-human-genome oligonucleotide microarray (version 2.0) G4845A (Agilent Technologies). Each microarray uses 44,495 probes to interrogate 27,958 Entrez gene RNAs. One hundred nanograms of total RNA was reverse transcribed into double-stranded cDNAs by AffinityScript multiple-temperature reverse transcriptase and amplified for 2 h at 40°C. The resulting cDNAs were subsequently used for *in vitro* transcription by the T7 polymerase and labeled with cyanine-3-labeled cytosine triphosphate (Perkin Elmer, Waltham, MA) for 2 h at 40°C using a low-input Quick-Amp labeling kit (Agilent Technologies) according to the manufacturer's protocol. After labeling, the rates of dye incorporation and quantification were measured with a Nanodrop ND-1000 (version 3.5.2) spectrophotometer (Thermo Scientific), and then the cRNAs were fragmented for 30 min at 60°C in the dark. Differentially labeled samples of 1,650 ng of cRNA were hybridized on Agilent 4 × 44K whole-genome arrays (version 2.0; 026652; Agilent Design) at 65°C for 17 h with rotation in the dark. Hybridization was performed using a gene expression hybridization kit (Agilent Technologies) following the manufacturer's instructions. After washing in gene expression washing buffer, each slide was scanned with the Agilent microarray scanner G2505C. Feature extraction software (version 10.5.1.1) employing defaults for all parameters was used to convert the images into gene expression data. Raw data were imported into a Subio platform (version 1.12) for database management and quality control. Raw intensity data were normalized against GAPDH (glyceraldehyde-3-phosphate dehydrogenase) expression levels for further analysis. These raw data have been accepted by GEO (a public repository for microarray data aimed at storing minimum information about microarray experiments [MIAME]).

Plasmids. The cDNA clones of wild-type (WT) and mutant (MT) pri-miR-122 and *Aequorea coerulescens* green fluorescent protein (AcGFP) were inserted between the XhoI and XbaI sites of lentiviral vector pCSII-EF-RfA, which was kindly provided by M. Hijikata, and the resulting plasmids were designated pCSII-EF-WT-miR-122, pCSII-EF-MT-miR-122, and pCSII-EF-AcGFP, respectively. Plasmids pHH-JFH1 and pSGR-JFH1, which encode full-length and subgenomic cDNA of the JFH1 strain, respectively, were kindly provided by T. Wakita. pHH-JFH1-E2p7NS2mt contains three adaptive mutations in pHH-JFH1 (53). pHH-JFH1-M1 and pHH-JFH1-M2 were established by the introduction of a point mutation of nucleotide 26 located in site 1 and nucleotide 41 in site 2 of the 5′ UTR of the JFH1 cDNA construct pHH-JFH1. pSGR-Con1, which encodes SGR of the Con1 strain, was kindly provided by R. Bartenschlager. The complementary sequences of miR-122 were introduced into the multicloning site of the pmirGLO vector (Promega, Madison, WI), and the resulting plasmid was designated pmirGLO-compl-miR-122. The plasmids used in this study were confirmed by sequencing with an ABI 3130 genetic analyzer (Applied Biosystems, Tokyo, Japan).

Cell lines. All cell lines were cultured at 37°C under the conditions of a humidified atmosphere and 5% CO_2. The following cells were maintained in Dulbecco modified Eagle medium (DMEM; Sigma-Aldrich, St. Louis, MO) supplemented with 100 U/ml penicillin, 100 μg/ml streptomycin, and 10% fetal calf serum (FCS): human hepatocellular carcinoma-derived Huh7, Hep3B, and HepG2; embryonic kidney-derived HEK293 and 293T; lung-derived RERF-LC-AI, NCI-H-2030, and A-427; kidney-derived Caki-2 and 769-P; neuron-derived MC-IXC and SK-PN-DW; uterus-derived Hec1B; ovary-derived SK-OV3; colon-derived SW620; and urinary bladder-derived SW780 cells. RERF-LC-AI (RCB0444) cells were provided by the RIKEN BRC through the National Bio-Resource Project of MEXT, Japan. Hec1B (JCRB1193) cells were obtained from the JCRB Cell Bank. NCI-H-2030, A-427, Caki-2, 769-P, MC-IXC, SK-PN-DW, SK-OV3, and SW780 cells were obtained from the American Type Culture Collection (ATCC). SW620 cells were kindly provided by C.

Oneyama. 293T-CLDN cells stably expressing CLDN1 were established by the introduction of the expression plasmids encoding CLDN1 under the control of the CAG promoter of pCAG-pm3. The Huh7-derived cell line Huh7.5.1 was kindly provided by F. Chisari. The Huh7OK1 cell line efficiently propagates HCVcc as previously described (45). Huh7, Hec1B, and HEK293 cells harboring Con1- or JFH1-based HCV SGR were prepared according to the method described in a previous report (47) and maintained in DMEM containing 10% FCS and 1 mg/ml G418 (Nakalai Tesque, Kyoto, Japan).

Antibodies and drugs. Mouse monoclonal antibodies to HCV nonstructural protein 5A (NS5A) and β-actin were purchased from Austral Biologicals (San Ramon, CA) and Sigma-Aldrich, respectively. Mouse anti-ApoE antibody was purchased from Santa Cruz Biotechnology (Santa Cruz, CA). Rabbit anti-HCV core protein and NS5A were prepared as described previously (41). Rabbit anti-SR-BI antibody was purchased from Novus Biologicals (Littleton, CO). Rabbit anti-CLDN1 and -OCLN antibodies, Alexa Fluor 488 (AF488)-conjugated anti-rabbit or -mouse IgG antibodies, and AF594-conjugated anti-mouse IgG2a antibodies were purchased from Invitrogen (San Diego, CA). Mouse anti-FKBP8 antibody was described previously (44). Mouse anti-double-stranded RNA (anti-dsRNA) IgG2a (J1 and K2) antibodies were obtained from Biocenter Ltd. (Szirak, Hungary). The HCV NS3/4A protease inhibitor was purchased from Acme Bioscience (Salt Lake City, UT). Human recombinant alpha IFN (IFN-α) and cyclosporine were purchased from PBL Biomedical Laboratories (Piscataway, NJ) and Sigma-Aldrich, respectively. BODIPY 558/568 lipid probe was purchased from Invitrogen. The locked nucleic acid (LNA) targeted to miR-122, LNA-miR-122 (5′-CcAttGTcaCaCtCC-3′), and its negative control, LNA-control (5′-CcAttCTgaCcCtAC-3′) (LNAs are in capital letters, DNAs are in lowercase letters; sulfur atoms in oligonucleotide phosphorothioates are substituted for nonbridging oxygen atoms; the capital C indicates LNA methylcytosine), were purchased from Gene Design (Osaka, Japan) (15).

Preparation of viruses. pHH-JFH1-E2p7NS2mt was introduced into Huh7.5.1 cells, HCVcc in the supernatant was collected after serial passages (39), and infectious titers were determined by a focus-forming assay and expressed in focus-forming units (FFUs) (62). Mutant HCVcc was produced from Huh7.5.1 cells expressing MT miR-122 according to the method of a previous report with minor modifications (25). HCVpv, a pseudotype vesicular stomatitis virus (VSV) bearing HCV E1 and E2 glycoproteins, was prepared as previously described (61), and infectivity was assessed by luciferase expression on a Bright-Glo luciferase assay system (Promega), following a protocol provided by the manufacturer and expressed in relative light units (RLUs).

Lipofection and lentiviral gene transduction. Cells were transfected with the plasmids by using Trans IT LT-1 transfection reagent (Mirus, Madison, WI) according to the manufacturer's protocol. LNAs were introduced into cells by Lipofectamine RNAiMAX (Invitrogen). The lentiviral vectors and ViraPower lentiviral packaging mix (Invitrogen) were cotransfected into 293T cells, and the supernatants were recovered at 48 h posttransfection. The lentivirus titer was determined by a Lenti-XTM quantitative reverse transcription-PCR (qRT-PCR) titration kit (Clontech, Mountain View, CA), and the expression levels of miR-122 and AcGFP were determined at 48 h postinoculation.

Quantitative RT-PCR. HCV RNA levels were determined by the method described previously (18). Total RNA was extracted from cells by using an RNeasy minikit (Qiagen). The first-strand cDNA synthesis and qRT-PCR were performed with TaqMan EZ RT-PCR core reagents and an ABI Prism 7000 system (Applied Biosystems), respectively, according to the manufacturer's protocols. The primers for TaqMan PCR targeted to the noncoding region of HCV RNA were synthesized as previously reported (42). To determine the expression levels of miR-122, total miRNA was prepared by using the miRNeasy minikit, and miR-122 expression was determined by using fully processed miR-122-specific RT and PCR primers provided in the TaqMan microRNA assays according to the manufacturer's protocol. U6 small nuclear RNA was used as an internal control. Fluorescent signals were analyzed with the ABI Prism 7000 system.

Immunoblotting. Cells were lysed on ice in lysis buffer (20 mM Tris-HCl [pH 7.4], 135 mM NaCl, 1% Triton X-100, 10% glycerol) supplemented with a protease inhibitor mix (Nacalai Tesque). The samples were boiled in loading buffer and subjected to 5 to 20% gradient SDS-PAGE. The proteins were transferred to polyvinylidene difluoride membranes (Millipore, Bedford, MA) and reacted with the appropriate antibodies. The immune complexes were visualized with SuperSignal West Femto substrate (Pierce, Rockford, IL) and detected with an LAS-3000 image analyzer system (Fujifilm, Tokyo, Japan).

Immunofluorescence assay. Cells cultured on glass slides were fixed with 4% paraformaldehyde (PFA) in phosphate-buffered saline (PBS) at room temperature for 30 min, permeabilized for 20 min at room temperature with PBS containing 0.2% Triton, after being washed three times with PBS, and blocked with PBS containing 2% FCS for 1 h at room temperature. The cells were incubated with PBS containing appropriate primary antibodies at room temperature for 1 h, washed three times with PBS, and incubated with PBS containing AF488- or AF594-conjugated secondary antibodies at room temperature for 1 h. For lipid droplet staining, cells incubated in medium containing 20 μg/ml BODIPY for 20 min at 37°C were washed with prewarmed fresh medium and incubated for 20 min at 37°C. Cell nuclei were stained with DAPI (4′,6-diamidino-2-phenylindole). Cells were observed with a FluoView FV1000 laser scanning confocal microscope (Olympus, Tokyo, Japan).

***In vitro* transcription, RNA transfection, and colony formation.** The plasmids pSGR-Con1 and pSGR-JFH1 were linearized with ScaI and XbaI, respectively, and treated with mung bean exonuclease. The linearized DNA was transcribed *in vitro* by using a MEGAscript T7 kit (Applied Biosystems) according to the manufacturer's protocol. The *in vitro*-transcribed RNA (10 μg) was electroporated into Hec1B and HEK293 cells at 10^7 cells/0.4 ml under conditions of 190 V and 975 μF using a Gene Pulser apparatus (Bio-Rad, Hercules, CA) and plated on DMEM containing 10% FCS. The medium was replaced with fresh DMEM containing 10% FCS and 1 mg/ml G418 at 24 h posttransfection. The remaining colonies were cloned by using a cloning ring (Asahi Glass, Tokyo, Japan) or fixed with 4% PFA and stained with crystal violet at 4 weeks postelectroporation.

Electron microscopy and correlative FM-EM analysis. Cells were cultured on a Cell Desk polystyrene coverslip (Sumitomo Bakelite) and were fixed with 2% formaldehyde and 2.5% glutaraldehyde in 0.1 M cacodylate buffer (pH 7.4) containing 7% sucrose. Cells were postfixed for 1 h with 1% osmium tetroxide and 0.5% potassium ferrocyanide in 0.1 M cacodylate buffer (pH 7.4), dehydrated in graded series of ethanol, and embedded in Epon812 (TAAB). Ultrathin (80-nm) sections were stained with saturated uranyl acetate and lead citrate solution. Electron micrographs were obtained with a JEM-1011 transmission electron microscope (JEOL). Correlative fluorescence microscopy (FM)-electron microscopy (EM) allows individual cells to be examined both in an overview with FM and in a detailed subcellular-structure view with EM (51). The NS5A was stained and observed in the Hec1B-derived Con1 SGR cells by the correlative FM-EM method as described previously (44).

Intracellular infectivity. Intracellular viral titers were determined according to a method previously reported (20). Briefly, cells were extensively washed with PBS, scraped, and centrifuged for 5 min at 1,000 × *g*. Cell pellets were resuspended in 500 μl of DMEM containing 10% FCS and subjected to three cycles of freezing and thawing using liquid nitrogen and a thermo block set to 37°C. Cell lysates were centrifuged at 10,000 × *g* for 10 min at 4°C to remove cell debris. Cell-associated infectivity was determined by a focus-forming assay.

Statistical analysis. The data for statistical analyses are averages of three independent experiments. Results were expressed as means ± standard deviations. The significance of differences in the means was determined by Student's *t* test.

Microarray data accession number. Access to data concerning this study may be found under GEO experiment accession number GSE32886.

RESULTS

Nonhepatic cell lines susceptible to HCVcc by expression of miR-122. Human CD81 (hCD81), SR-B1, CLDN1, and OCLN are crucial for HCV entry (16, 48, 49, 56). First, we examined the expression of these receptor candidates in nonhepatic cell lines by using the web-based NextBio search engine (Cupertino, CA). Multidimensional scaling was used to visualize the differences in expression patterns of molecules of various tissues, cells, and cell lines from those of hepatic cell lines and primary hepatocytes. We selected nine nonhepatic cell lines as possibly being susceptible to HCVcc infection: NCI-H-2030 (lung), Caki-2 (kidney), 769-P (bladder), A-427 (lung), SK-OV3 (ovary), SW780 (bladder), SW620 (colon), RERF-LC-AI (lung), and Hec1B (uterus) (Fig. 2). In addition, three nonhepatic cell lines previously reported to be susceptible to replication of HCV RNA—that is, SK-PN-DW (neuron), MC-IXC (neuron), and 293T-CLDN (kidney)—were included in this study (8, 17). The expression of each receptor molecule in these 12 nonhepatic cell lines was confirmed by fluorescence-activated cell sorter (FACS) analysis and immunoblotting (Fig. 3A and B). To examine the expression of the functional receptors for HCV entry in these cell lines, we inoculated HCVpv into the cells. Ten of the cell lines (A-427 and SW780 being the exceptions) exhibited various degrees of susceptibility to HCVpv infection (Fig. 3C). Therefore, we examined the possibility of propagation of HCVcc by the expression of miR-122 in these 10 cell lines.

To introduce miR-122 in the cell lines, we employed a lentiviral vector encoding pri-miR-122, an unprocessed miR-122. To confirm the maturation of pri-miR-122 to form functional RNA-induced silencing complexes (RISCs), suppression of the translation of the target mRNA was determined by a dual reporter assay. Translation of a firefly luciferase mRNA containing the sequences complementary to miR-122 in the 3′ UTR was suppressed by infection with the lentivirus encoding pri-miR-122 but not by infection with a control virus (data not shown), suggesting that the pri-miR-122 is processed into a functionally mature miR-122. By using this lentiviral vector, high levels of miR-122 expression were achieved in the 10 cell lines, comparable to the endogenous expression level of miR-122 in Huh7 cells (Fig. 4A).

To examine the effect of the exogenous expression of miR-122 on HCV replication, the nonhepatic cell lines expressing miR-122 were infected with HCVcc at a multiplicity of infection (MOI) of 1, and intracellular viral RNA was determined (Fig. 4B). The expression of miR-122 significantly increased the amount of the HCV genome in Hec1B, 293T-CLDN, MC-IXC, and RERF-LC-AI cells as well as Huh7 cells and slightly increased it in SK-OV3 and NCI-H-2030 cells. Although the levels of viral RNA in SW620, Caki-2, and SK-PN-DW cells upon expression of miR-122 were higher than those in control cells, no increase of viral RNA was observed. No effect of the expression of miR-122 was observed in 769-P cells. Interestingly, naïve Hec1B cells exhibited a delayed increase in viral RNA from 24 to 48 h postinfection, in contrast to the gradual decrease of viral RNA in other cell lines. Replication of HCV RNA in both naïve and miR-122-expressing Hec1B cells was inhibited by treatment with an inhibitor for HCV protease but not by treatment with IFN-α, due to the lack of an IFN receptor (11), whereas treatments with either IFN-α or the protease inhibitor suppressed the replication of HCV in the other cell lines expressing miR-122 (Fig. 4C). These results indicate that exogenous miR-122 expression enhances the replication of HCV even in nonhepatic cells. Hec1B cells exhibit a delayed replication of HCV, and HCV replication was enhanced by the exogenous expression of miR-122. Therefore, in this study we used Hec1B cells to investigate the biological significance of miR-122 on the replication of HCVcc in nonhepatic cells.

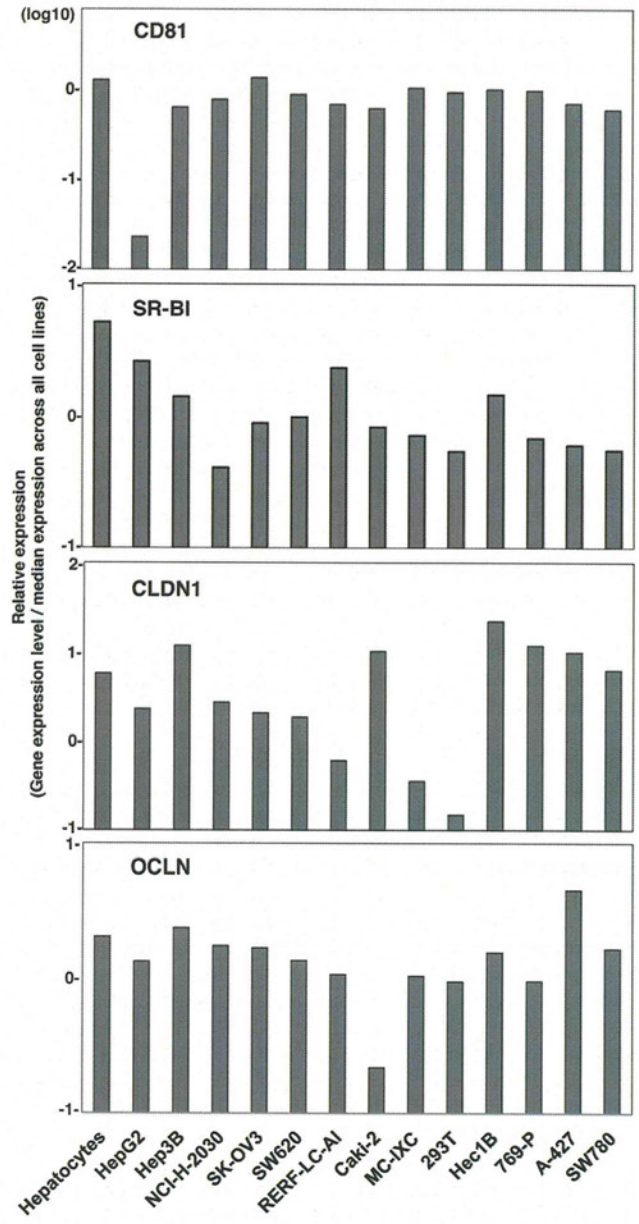

FIG 2 Receptor expression profiling in nonhepatic cells. Relative expression levels of CD81, SR-BI, CLDN1, and OCLN in primary hepatocytes, hepatic cell lines HepG2 and Hep3B, and nonhepatic cells were determined by using the NextBio Body Atlas. Expression levels were standardized by the median expression across all cell lines.

Expression of miR-122 is essential for enhancing HCV replication in Hec1B cells. To confirm the specificity of HCV replication in Hec1B cells, HCVcc was preincubated with an anti-HCV E2 monoclonal antibody, AP-33, or Hec1B/miR-122 and Hec1B/

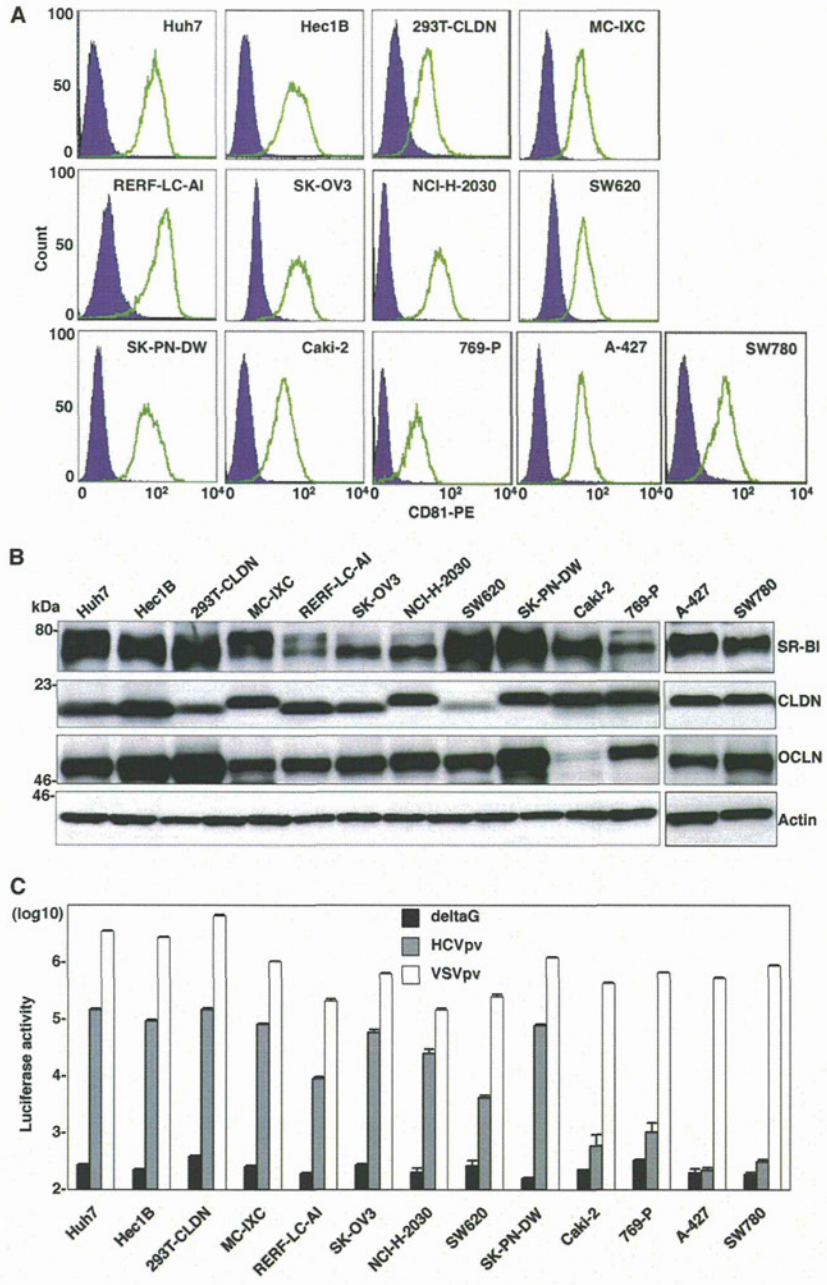

FIG 3 Expression of functional HCV receptor candidates in nonhepatic cells. (A) Expression of hCD81 in nonhepatic cells was determined by flow cytometry. PE, phycoerythrin. (B) Expression levels of SR-B1, CLDN, and OCLN in the nonhepatic cells were determined by immunoblotting. (C) The nonhepatic cell lines were inoculated with pseudotype VSVs bearing no envelope protein (deltaG), HCV envelope proteins of genotype 1b Con1 strain (HCVpv), or VSV G protein (VSVpv), and luciferase expression was determined at 24 h postinfection.

Cont cells were pretreated with anti-hCD81 monoclonal antibody. Replication of HCV RNA was determined upon infection with HCVcc. The antibody treatment significantly inhibited HCV replication in the Hec1B cell line, indicating that HCVcc internalizes into Hec1B cells through a specific interaction between hCD81 and E2 (Fig. 5). Next, we determined the dose dependence of miR-122 expression on the enhancement of HCV replication in Hec1B cells. Huh7.5.1 and Hec1B cells transduced with the lentiviral vector encoding pri-miR-122 were infected with HCVcc at an MOI of 1, and intracellular miR-122 and viral RNA were determined. Expression of miR-122 was increased in Hec1B cells in a dose-dependent manner of the lentivirus, whereas no increase was observed in Huh7.5.1 cells, probably due to the high level of endogenous expression of miR-122 (Fig. 6A, left). HCV RNA replication in Huh7.5.1 and Hec1B cells was correlated with miR-122 expression (Fig. 6A, right), suggesting a close correlation between miR-122 expression and HCV replication.

Next, we examined the expression of viral proteins in Hec1B/

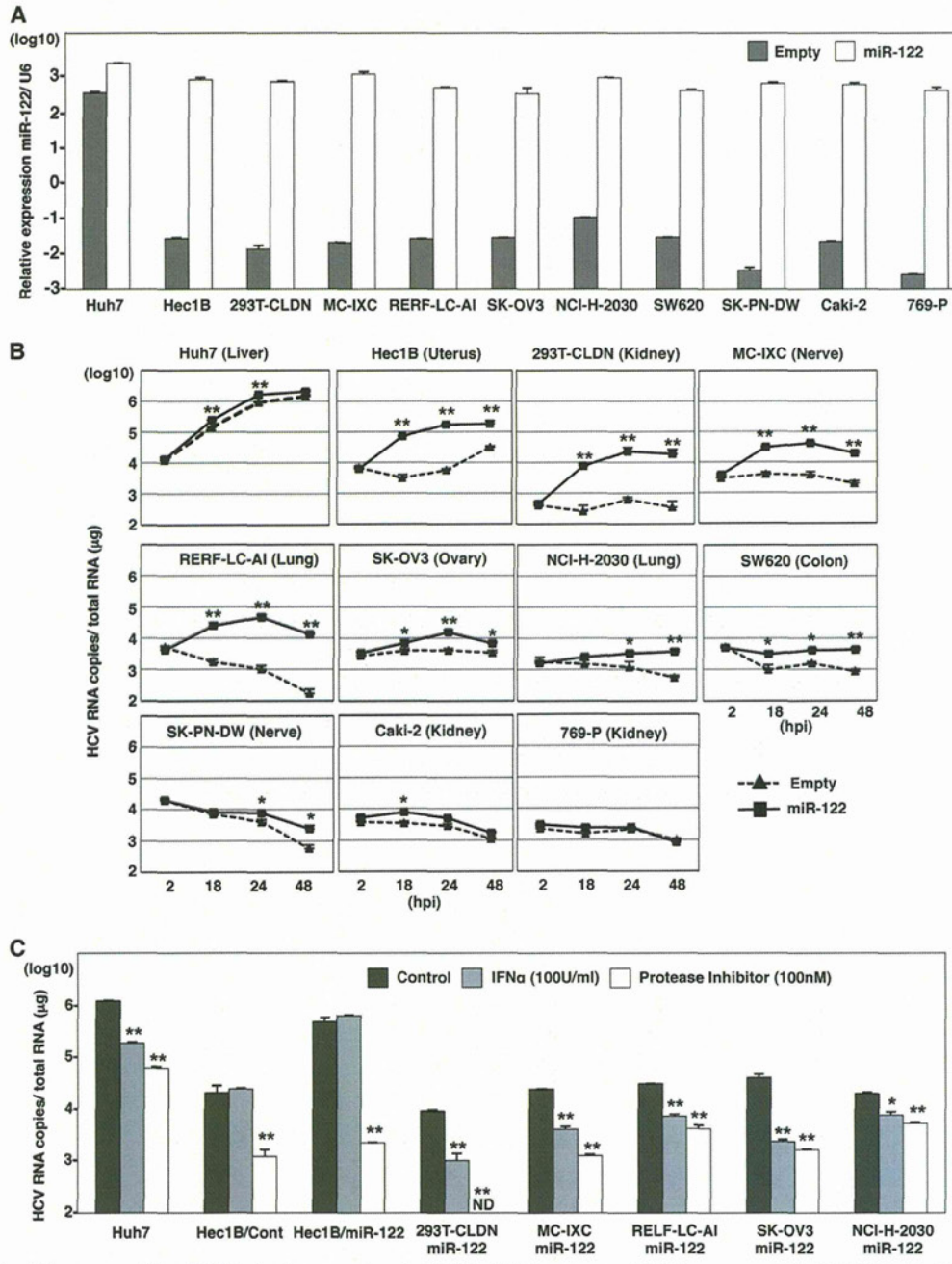

FIG 4 Nonhepatic cell lines susceptible to HCVcc by the expression of miR-122. (A) Exogenous miR-122 was expressed in Huh7, Hec1B, 293T-CLDN, MC-IXC, RERF-LC-AI, SK-OV3, NCI-H-2030, SW620, Caki-2, SK-PN-DW, and 769-P cells by lentiviral vector. Total RNA was extracted from the cells and subjected to qRT-PCR analysis. U6 was used as an internal control. Gray and white bars, endogenous and exogenous levels of miR-122, respectively. (B) HCVcc was inoculated into Huh7 and nonhepatic cell lines expressing (solid lines) or not expressing (dashed lines) exogenous miR-122 at an MOI of 1. Intracellular HCV RNA levels were determined by qRT-PCR at 2, 18, 24, and 48 h postinfection (hpi). (C) Cells were inoculated with HCVcc and simultaneously treated with either 100 U IFN-α or 100 nM HCV protease inhibitor or not treated (control), and intracellular HCV RNA levels were determined by qRT-PCR at 36 h postinfection. Asterisks indicate significant differences (*, $P < 0.05$; **, $P < 0.01$) versus the results for control cells.

miR-122 cells upon infection with HCVcc by immunoblotting and fluorescence microscopic analyses (Fig. 6B). Expression of NS5A protein was increased in Hec1B/miR-122 cells in an MOI-dependent manner. Expression of NS5A in Hec1B/Cont cells infected with HCVcc at an MOI of 3 was significantly lower than that in Hec1B/miR-122 cells infected with HCVcc at an MOI of 0.5. HCV core and NS proteins were shown to localize mainly on the lipid droplets and cytoplasmic face of the endoplasmic reticulum (ER) in Huh7 and Hep3B/miR-122 cells infected with HCVcc (29, 40). Immunofluorescence analyses revealed that HCV core and NS5A proteins were colocalized with lipid droplets and calnexin, an ER marker, in Hec1B cells infected with HCVcc (Fig. 7).